

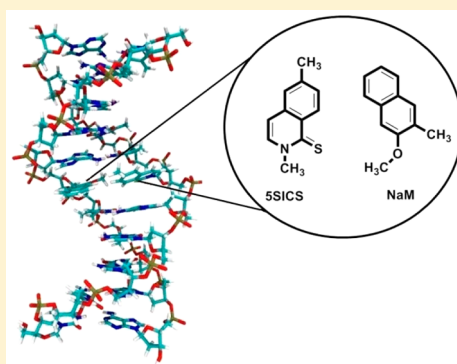
# What Sustains the Unnatural Base Pairs (UBPs) with No Hydrogen Bonds

Sk Jahiruddin and Ayan Datta\*

Department of Spectroscopy, Indian Association for the Cultivation of Science, 2A and 2B Raja S. C. Mullick Road, Jadavpur, 700032 Kolkata, West Bengal, India

## Supporting Information

**ABSTRACT:** The recent report of a hydrophobic unnatural base pair (UBP), d5SICS-dNaM, which replicated in DNA PCR and also sustained and synthesized a plasmid inside *E. coli* genome by Romesberg and coworkers, is intriguing. Quantum chemical calculations show that the UBPs prefer a slipped parallel configuration to facilitate weak dispersion interactions somewhat similar to the so-called  $\pi$ -stacking interaction. Nevertheless, within a natural DNA tract, classical molecular dynamics simulations show that the backbone and neighboring stacked bases together reorient the UBPs in natural base pair like planar environment. Our computed structure with an average end-end distance,  $d_{C1'-C1'} = 10.7$  Å for d5SICS-dNaM is in excellent agreement with available crystal structure (PDB ID: 3SV3, planar UBP with  $d_{C1'-C1'}^{\text{crystal}} = 11.0$  Å). Quantum mechanical calculations for the UBP flanked by two natural base-pairs (A–T) on top and on bottom on equilibrated MD structure found large binding energy ( $\Delta E = -74.0$  kcal/mol). The present calculations therefore establish the fact that the hydrophobic UBPs can be stabilized by dispersion interactions with other base pairs in the DNA tract even in the absence of any hydrogen bonding between the UBPs themselves.



## INTRODUCTION

The sequence and specificity of the nucleic acid base pairs in DNA/RNA define the eventual structure and functions of proteins. The underlying principle for the preservation of the genetic traits during replication arises from the selectivity of base pairing via N–H...O and N–H...N hydrogen bonding. Any other combination amounts to a mismatch, which if not repaired by proofread enzymes before protein synthesis leads to mutations. Nevertheless, there has been focused research toward the synthesis of unnatural base pairs that can possibly be incorporated into natural DNA tracts and replicated. This has important implications for designing new synthetic biomaterials, DNA base sensors, machines, and drug delivery systems as well as expanding the genetic alphabet that may then be permuted to make new words (molecules) that would be impossible from just the five natural bases.<sup>1–5</sup> On the basis of noncanonical patterns of H bonding between natural base pairs, Benner and coworkers have designed a large library of synthetic base pairs, which efficiently replicated.<sup>6</sup> Kool and coworkers introduced the concept of nonpolar nucleoside isosteres for molecules that have shape and volume similar to the natural bases but lack H-bonding motifs.<sup>7</sup> The hydrophobic base pairs of Hirao and coworkers retained excellently (97%) after 100 cycles of PCR.<sup>8</sup>

Another important application of base pairs has been to design pH-sensitive DNA-based switches that undergo transformation from a closed-loop-like structure at low pH to open-chain structure in high pH.<sup>9</sup> DeRosa and coworkers have

incorporated a A...G mismatch inside a DNA loop, which under acidic conditions undergo pairing through the AH<sup>+</sup>...G pair.<sup>10</sup> On the basis of tagging the stem loop structures with Cy3/Cy5 FRET pair, they observed reversible “on” and “off” pH-dependent cycles. On the basis of quantum chemical calculations, we have shown that even though in the gas phase for free bases, proton affinity of the N7 site of guanine is more than the N3 site of adenine; within the protonated A...G pair, the N3 site of adenine gets protonated to form AH<sup>+</sup>...G pair.<sup>11</sup> Preservation of planarity of the base pair on protonation has been elucidated as an important parameter for the overall stability of the 3D structure of modified DNA.

Recently, Romesberg and coworkers have reported the synthetic design of *E. coli* bacteria that contains hydrophobic UBPs and d5SICS-dNaM (Figure 1a) within its DNA and is able to sustain and replicate under intracellular conditions.<sup>1</sup> The robustness of the d5SICS-dNaM UBP led to accurate replication with no apoptosis as this pair is not recognized as a mismatch by the DNA repair mechanisms. Therefore, clearly this d5SICS-dNaM pair is an interesting system and a molecular level understanding of the forces that sustain this UBP merits an atomistic simulation. We have deciphered that the stability of this pair arises from the rather strong dispersion interactions between the planar d5SICS-dNaM pair with neighboring

**Received:** April 6, 2015

**Revised:** April 16, 2015

**Published:** April 20, 2015



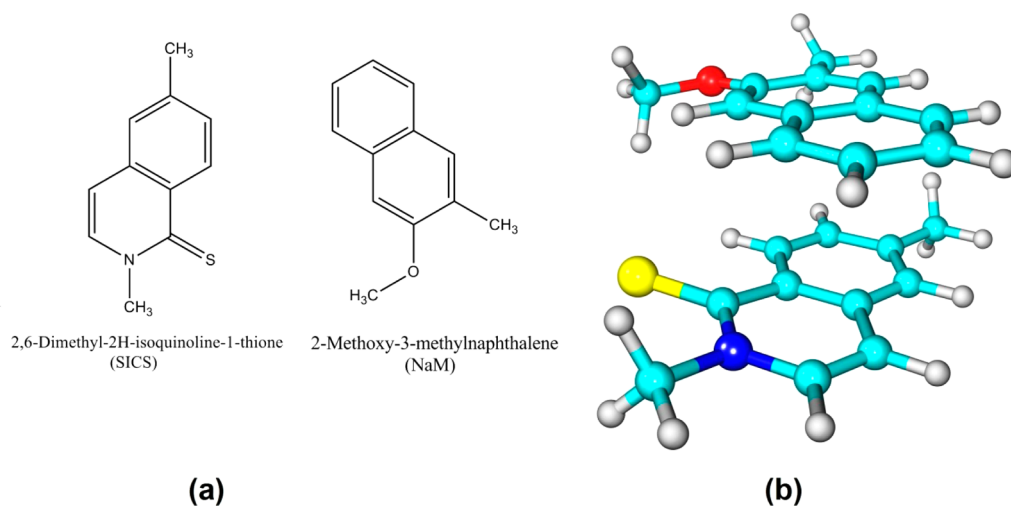


**Figure 1.** (a) Chemical structure of the SSICS and NaM bases. (b) Optimized structure of the SSICS-NaM pair (at M06-2X/aug-cc-pVDZ level of theory).

**Table 1. Binding Energies of SSICS-NaM Pair Using Different Levels of Theory**

method		binding energy (kcal/mol)	BSSE-corrected binding energy (kcal/mol)
DFT without medium range electron correlations	B3LYP/aug-cc-pVDZ	4.9	7.5
	PBE1PBE/aug-cc-pVDZ	−0.9	2.1
DFT - functionals with medium range electron correlations	M06-2X/aug-cc-pVDZ	−14.0	−11.0
	M06-2X/Def2TZVPP	−10.7	−10.1
DFT with Grimme's empirical dispersion	B3LYP-D3/aug-cc-pVDZ	−13.1	−10.5
	PBEPBE-D3/aug-cc-pVDZ	−12.9	−10.2
	PBE1PBE-D3/aug-cc-pVDZ	−13.1	−10.1
	PBE1PBE-D3BJ/aug-cc-pVDZ	−14.1	−11.1
	PBE1PBE-D3BJ/Def2TZVPP	−11.4	−10.8
	$\omega$ B97XD/aug-cc-pVDZ	−15.2	−12.6
	$\omega$ B97XD/Def2TZVPP	−12.5	−12.0
	HF/aug-cc-pVDZ	7.4	11.1
wave function methods	MP2/aug-cc-pVDZ	−29.9	−17.3
	RI-MP2/aug-cc-pVDZ	−29.5	−17.1
	RI-MP2/aug-cc-pVTZ	−23.4	−18.3
	RI-SCS-MP2/aug-cc-pVDZ	−23.4	−10.8
	RI-SCS-MP2/aug-cc-pVTZ	−17.3	−11.9
	RI-SCS-MP2/Def2TZVPP	−14.4	−10.4

stacked bases. On the basis of quantum chemical and classical molecular dynamics simulations, we have shown that incorporation of the dSSICS-dNaM UBP does not hamper the stability and double-helical structure of DNA. In fact, the C1'–C1' distances of UBP-modified DNA are similar to that for the Watson–Crick pairs. Clearly, intrastrand stacking interactions within the sugar–phosphate backbone seem to be more important than the individual interstrand hydrogen bonding (or the lack of it in the UBP).

## COMPUTATIONAL DETAILS

For quantum chemical calculations, the structure of the SSSICS-NaM pair as well as individual bases was optimized at the M06-2X/aug-cc-pVDZ level,<sup>12</sup> followed by harmonic frequency calculations that were performed to ensure the absence of vibrational instabilities. Single point energy calculations were performed using various level of theory on the M06-2X-optimized structures. Close proximity of Truhlar's M06-2X meta-GGA-hybrid functional with benchmark databases has been previously reported in literature for a wide

variety of molecular complexes.<sup>13,14</sup> According to previous benchmarks we expect the M06-2X and  $\omega$ B97XD functional to give the most accurate DFT binding energies.<sup>15,16</sup> For the ONIOM calculations, the high layer consisting of the UBP along with the linked sugars and phosphates was performed at the M06-2X/6-31+(d) level, while the low layer consisting of the four natural base pairs above and below the UBP inclusive of their link sugars and phosphates was performed at the semiempirical PM3 level. Neutrality of the overall system was ensured by protonation of the eight PO<sub>4</sub> ions and the four oxygen atoms attached to the deoxyribose rings at either end of the sequence. All quantum chemical calculations were performed on Gaussian 09<sup>17</sup> and ORCA 3.0.1.<sup>18</sup>

For classical molecular dynamics simulation, the unnatural base pair (UBP) has been parametrized by extensive quantum mechanical calculations and CHARMM CGenFF 2b8 force field.<sup>19</sup> Partial charges were generated with MP2 charge density and modified according to standard CHARMM conventions.<sup>20</sup> The partial charges and parameters were validated by energy minimization of the individual SSICS-NaM pair, which leads to

comparable binding energy and structures as obtained from quantum chemical calculations, as discussed in Table 1. (See the Supporting Information (SI) for calibration of the parameters for SSICS and NaM and details of MD simulations.) Initial coordinates of 5'-TCACAXTTCCA-3' sequence were retrieved from the make-na automated generator,<sup>21,22</sup> and a natural pair was replaced by SSICS-NaM. The inherent negative charges arising from the 22 inorganic phosphates were neutralized by placing 22 sodium ions inside the water box. All simulations were performed in NAMD 2.9.<sup>23</sup> Molecular visualization and analyses were performed in VMD 1.9.<sup>24</sup>

## ■ RESULTS AND DISCUSSION

**1. Quantum Chemistry.** Figure 1b shows the optimized structure of the free SSICS-NaM pair; each base is terminated by a methyl group from sugar phosphate backbone at the M06-2X/aug-cc-pVDZ level of theory. The molecules are oriented in a slipped parallel orientation with center-to-center distance of 3.59 Å. (See Table S1 in the SI for binding energy of the pair as a function of stacking distance.) The distance between the H atom of the methoxy group in 2-methyl, 3-methoxynaphthalene (NaM) and the S atom of the thione group in 2,6-dimethyl-2H-isoquinoline-1-thione (SSICS) is 3.25 Å, which exceeds the sum of their van der Waals radii ( $r_{\text{vdW}}^{\text{H}} + r_{\text{vdW}}^{\text{S}} = 3.0$  Å),<sup>25</sup> thereby eliminating the role of a weak C(d+)-H(d+)...S(d-)=C(d+) type hydrogen-bonding interaction in stabilizing the slipped parallel configuration of the SSICS-NaM pair. The optimized structure for the pair was used to determine the binding energies at various single-point levels. Table 1 reports the basis set superposition error (BSSE)-corrected binding energies for the pair at different levels of theory.

The interactions between the hydrophobic SSICS-NaM pair are different from the natural H-bonded base pairs like A-T and G-C having binding energies of -15.4 and -28.8 kcal/mol at the CCSD/CBS level.<sup>26</sup> Clearly, the nonpolar SSICS-NaM pair shares similar traits as those for intermolecular interactions between alkane chains or aromatic molecules like benzene dimer.<sup>27-29</sup> Consideration of medium-range electron correlations at the M06-2X/aug-cc-pVDZ level leads to significant binding energy (BSSE corrected) = -10.9 kcal/mol. Incorporation of empirical dispersion interactions within the Grimme's DFT-D3 level also predicts very similar binding energies. Møller-Plesset second-order perturbation (MP2) calculations also predict a highly stable complex where the binding energies are probably overestimated.<sup>30</sup> Improving the basis set from aug-cc-pVDZ to aug-cc-pVTZ followed by the spin-component scaled MP2 (SCS-MP2)<sup>31</sup> led to a better agreement with the M06-2X/DFT-D3 results. Therefore, the binding energy for the SSICS-NaM pair should be in between -10.0 and -12.0 kcal/mol according to our best estimates. Apart from SSICS-NaM interactions, SSICS and NaM molecules are also shown to undergo effective  $\pi$ -stacking interactions with natural bases like A, T, G, and C. Both SSICS and NaM were optimized, placing the natural bases at a stacking distance of 3.4 Å, which corresponds to the distance between the stacked bases in canonical DNA. The optimized structures remained stacked as in the natural environment and lead relatively large complexation energies,  $\Delta E_{\text{stack}} = -11.9$ , -13.6, -13.2, and -10.3 kcal/mol for NaM...A, NaM...G, NaM...T, and NaM...C and -12.7, -19.9, -13.0, and -14.6 kcal/mol for SSICS...A, SSICS...G, SSICS...T, and SSICS...C, respectively, at the  $\omega$ B97XD/DefT2ZVPP level

of theory. The stacking interaction energies between the UBPs and the natural bases are relatively larger than binding energies of the natural stacked bases.<sup>32-34</sup> The large binding energies of SSICS and NaM with the natural stacked bases play a significant role in stabilizing the overall DNA double-helix structure.

**2. Effects of Solvation and Potential of Mean Force Calculations.** The unique nature of interactions that stabilize the SSICS-NaM pair in comparison with the natural base pairs can be adjudged by the rather small penalty paid on solvation in aqueous medium. The binding energy for the SSICS-NaM pair decreases from -10.7 kcal/mol in gas phase to -8.2 kcal/mol in water (at the CPCM model<sup>35</sup>) at the M06-2X/aug-cc-pVDZ level of theory, a depreciation of only 23%. A similar picture is also obtained at other levels of theory. In contrast, the natural base pairs exhibit a much larger decrease in their binding energies on solvation (~34 and 45% for A-T and G-C, respectively; see Table S2, SI). The large decrease in the binding energies for natural hydrogen bonded pairs on solvation can be understood by the fact that on solvation both the hydrogen bond donors and acceptors are separately solvated (screened), thereby reducing the efficacy of the electrostatic interactions involved in the intermolecular hydrogen bonding.<sup>36,37</sup> On the basis of a detailed analysis of the variation of the binding energy ( $\Delta E$ ) of the A-T base-pair with respect to the dielectric constant ( $\epsilon$ ), it has been previously shown that  $\Delta E$  decreases exponentially with  $\epsilon$ , which can be analytically expressed in terms of a charging of a capacitor model;<sup>38</sup> however, the solvation behavior of the SSICS-NaM is remarkably different as there are hardly any hydrogen bond donors or acceptors on the individual bases that can be efficiently solvated. The small decrease in the binding energy for the SSICS-NaM pair on solvation probably arises from the partial screening of the charge densities of the electronegative atoms like sulfur and oxygen in SSICS and NaM, respectively.

One crucial drawback of the implicit solvation models within quantum chemistry is the lack of explicit polarization of solutes by the solvents in the immediate vicinity. A more reasonable estimate of the association affinity of two molecules in water can be undertaken by evaluating the free energy of association as a function of their center-to-center distance through potential of mean force (PMF) calculations. The center-to-center distance of the SSICS-NaM pair was defined as the reaction coordinate along which PMF was estimated using classical MD simulations at 310 K. The reaction coordinate was divided into three windows both of 4 Å widths to collect the data from 2.4 to 14.4 Å for 10 ns for each window. Figure 2 shows the PMF of the SSICS-NaM pair as a function of the intermolecular center-to-center distance, where PMF at  $d_{\text{center-to-center}} = 14.4$  Å is scaled to zero. The plot has a minimum for  $d_{\text{center-to-center}} = 3.9$  Å and free energy of association,  $\Delta G_{\text{association}} = -3.5$  kcal/mol. The computed free energy of association for the SSICS-NaM pair is found to be similar to that for the natural stacked bases like A and T in water.<sup>39</sup>

**3. QM:PM3 and Classical Molecular Dynamics.** The SSICS-NaM pair was incorporated inside a short double-stranded DNA sequence consisting of 5'-CAXTT (complementary: 3'-GTYAA) where X = SSICS and Y = NaM to probe the structure and orientation of the UBP inside the double helix. A multiscale ONIOM (QM:PM3) method was used to optimize this short sequence.<sup>40</sup> Compared with the gas-phase structures of the dimer (Figure 1b), the structure of UBP



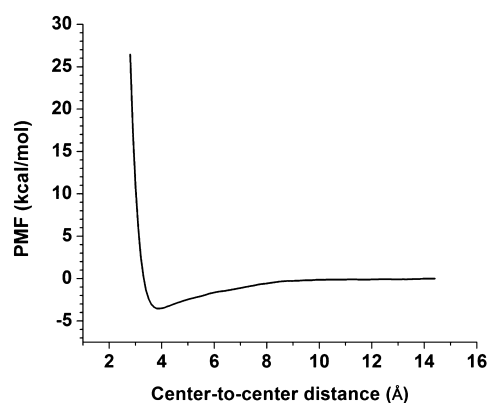


**Figure 2.** Potential of mean force (PMF) as a function of the center–center distance for the SICS–NaM pair in explicit water at 300 K.

incorporated inside the DNA tract shows interesting variations (Figure 3, inset). Within the tract, the UBPs are no longer

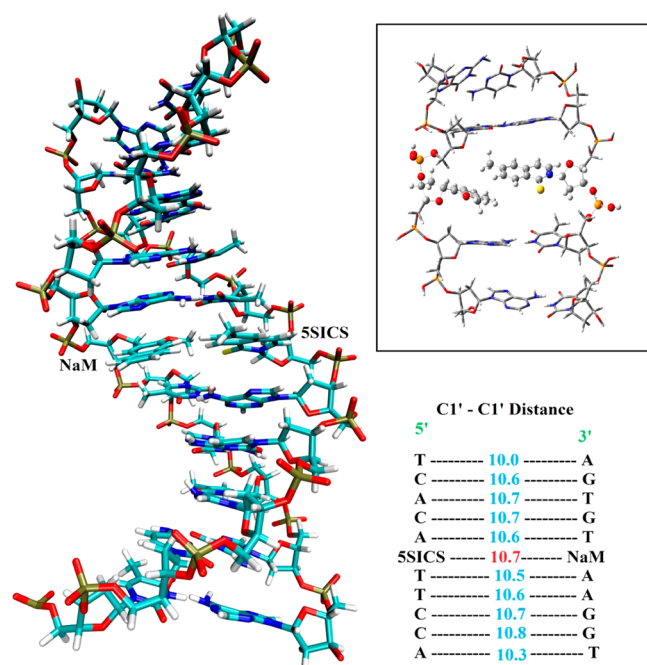


**Figure 3.** MD snapshot of the DNA sequence with unnatural base pair after 177 ns of production run. Inset: Optimized structure (M06-2X/6-31G(d):PM3 level) of the pair inside a short DNA tract.

stacked with respect to each other and tend to orient themselves within a planar orientation so as to maximize  $\pi$ -stacking with the natural bases above and below the UBP. Because the QM:PM3 calculations did not reveal any new bond formation or dissociation when the UBP is planted inside DNA, we expect that classical molecular dynamics should be able to describe the average room temperature structure including orientation of the natural and unnatural base pairs and stability of UBP@DNA in explicit water/counterion environment.

We performed 250 ns of NVT classical molecular dynamics simulation of a short DNA sequence of 5'-TCACAXTTCCA-3' analogous to the experimental one<sup>1</sup> inside a water box of dimension  $50 \times 50 \times 66 \text{ \AA}^3$  using CHARMM27<sup>41</sup> force field. A careful multistep equilibration protocol was adapted as the stability of the system is the topic of interest. The system was

minimized for 10 000 steps first while keeping the DNA atoms restrained by a force of  $100 \text{ kcal/\AA}^2$ . Then, the system was minimized for another 10 000 steps without applying any restraint to any atom. After minimization the system was equilibrated for 5 ns with a restrained force of  $100 \text{ kcal/\AA}^2$  on DNA atoms. Then, the restrained force was reduced to  $20 \text{ kcal/\AA}^2$  and the system was equilibrated for another 5 ns. Finally, the fully relaxed system was equilibrated for 15 ns in NPT ensemble at 310 K. The UBPs were parametrized using CHARMM General Force Field (CGenFF 2b8) and extensive quantum chemical (MP2) calculations.<sup>19,20</sup> The DNA sequence along with UBP remained stable throughout the 250 ns of production run. Strikingly, the UBP starts to resemble the natural base pairs as they become quasiplanar with respect to each other. The planarity of the 5SICS–NaM pair within DNA ensures effective stacking with the natural base pairs present above and below the UBP.

Figure 3 shows a snapshot of UBP@DNA after 174 ns of production run. Clearly, the dSICS–dNaM pair and the natural base pairs are indistinguishable both in terms of planarity and the end-to-end C1'–C1' distances. The mean computed  $d_{\text{C1'–C1'}}$  is  $10.7 \text{ \AA}$  for UBP, which is similar to that for the natural bases in the tract. Figure 4 shows the time evolution of C1'–C1' distance between the complementary residues in the system except the first and last residues. First and last residues were omitted as the last residues fluctuated more in the absence of other stacked pairs in the opposite side. As expected, even the second to last residues (shown as Figure 4a,i) fluctuated more than the other internal residues. Mean and time evolution of  $d_{\text{C1'–C1'}}$  confirms that the DNA was stable and the double-helix structure was preserved throughout the simulation.

To probe further the effects of neighboring stacked bases on the stability of the DNA, we calculated the center-to-center distances of NaM and 5SICS with their intrastrand stacked neighboring bases. The average center-to-center distances of the 5SICS–adenine (above) and 5SICS–thymine (below) stacking distances are  $3.9$  and  $4.7 \text{ \AA}$ , respectively, while those for NaM–thymine (above) and NaM–adenine (below) stacking distances are  $4.2$  and  $3.7 \text{ \AA}$ , respectively, which are similar to those for the stacked natural bases. Figure 5 shows the time evolution of the center-to-center distances of the 5SICS–NaM pair with their neighboring stacked bases. Our predicted planar dSICS–dNaM within a natural DNA tract is in excellent agreement with the crystal structure of KlenTaq DNA polymerase containing the UBP ( $d_{\text{C1'–C1'}}^{\text{crystal}} = 11.0 \text{ \AA}$ ), which exhibited efficient replication and selectivity.<sup>42</sup> The agreement of our simulation data with the crystal structure data substantiates the experimental hypothesis that the DNA replication enzymes requires a planar WC type base-pair geometry and the absence of H-bonding interactions in UBP does not deter DNA replication.<sup>43</sup>

To clearly the decipher the stability afforded to DNA by the hydrophobic UBP pair, we also ran an MD simulation on void incorporated sequence, namely, 5'-TCACAΦTTCCA-3', where Φ represents an absence of the UBP. The sugar–phosphate backbone was, however, maintained to ensure nonfragmentation of the sequence, and a similar MD protocol as previously mentioned for UBP@DNA was used. Figure 6 shows the representative MD snapshot after 177 ns of production run. Large structural distortions are evident near the void. The C1'–C1' distance increases to  $21.5 \text{ \AA}$ , indicating the instability of such a configuration. Interestingly, while the UBP remains symmetrically placed inside the DNA with the

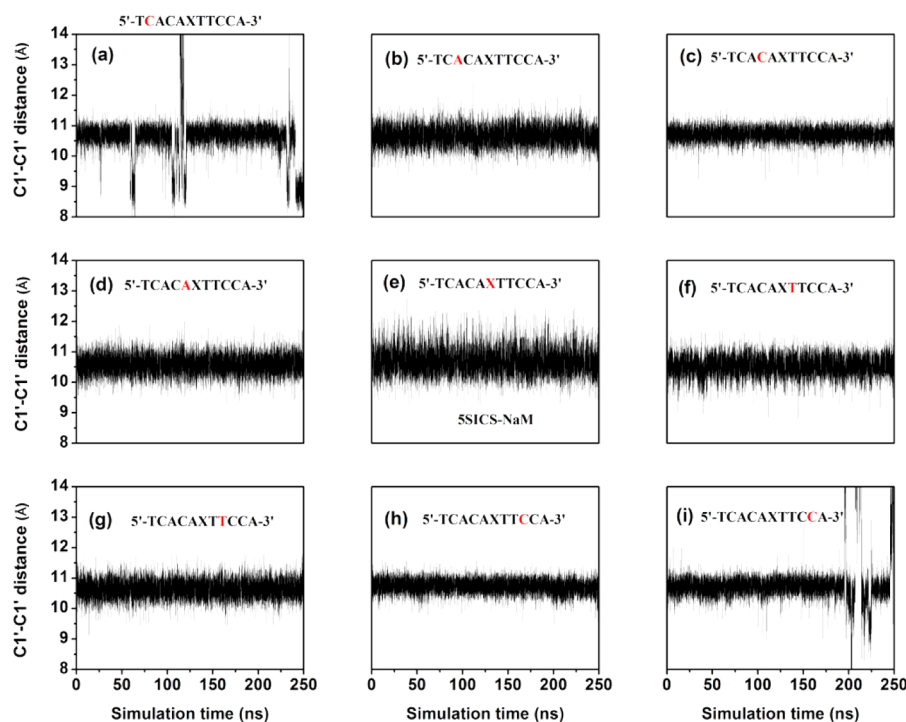


**Figure 4.** Time evolution of the C1'–C1' distances for natural and unnatural residues as in the retrieved sequence 5'-TCACAXTTCCA-3'. (The highlighted letter in each of the Figure shows the respective position of the residue in the sequence.)

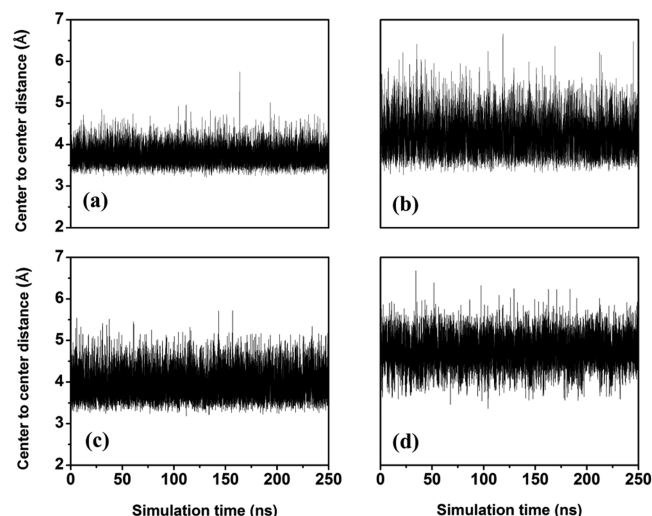


**Figure 5.** Time evolution of the center-to-center distances between unnatural base and their neighboring stacked natural bases. (a) NaM-adenine, (b) NaM-thymine, (c) 5SICS-adenine, and (d) 5SICS-thymine.

center-to-center distance of  $\sim 8.0$  Å between the top and bottom stacked natural bases on either end, a void creates asymmetry in the stacking pattern. The UBP therefore provides an excellent stacking profile to maintain the double-helical pattern of DNA.

To probe the true nature of stability of the UBP inside the double helix further we isolated a triple pair from the experimental sequence, namely, natural–unnatural–natural consisting of two A–T pairs at upper and lower ends and 5SICS–NaM in middle from the 20 ns equilibrated MD structure and calculated energies of the whole structure as well as individual bases. (See Figure 7.) The binding energy was

found to be  $-78.5$  kcal/mol (BSSE-corrected binding energy =  $-74.0$  kcal/mol) at the  $\omega$ B97XD/Def2TZVP level of theory. (See Table S3, SI.) It is important to note that even though the 5SICS–NaM pair loses its higher stability arising out of mutual  $\pi$ -stacking interactions, it is overcompensated by the presence of strong hydrogen bonding interactions between the two A–T pairs that therefore enforces a planar UBP. Nevertheless, a significant binding energy confirms that apart from hydrogen bonding interactions between the natural pairs van der Waals interactions between the stacked natural and unnatural bases contribute significantly toward stabilizing a UBP within DNA.

## CONCLUSIONS

Quantum chemical and classical molecular dynamics calculations reveal the interaction patterns among the 5SICS–NaM pair. As expected, in the absence of any hydrogen-bonding interaction between them, the gas-phase structure of the dimer is a stacked configuration with a center-to-center distance of 3.59 Å and binding energy of approximately  $-10.0$  to  $-12.0$  kcal/mol. In the presence of explicit water molecules, PMF calculations reveal a free energy of association of  $-3.5$  kcal/mol at 310 K. Nevertheless, classical molecular dynamics simulations for the 5SICS–NaM pair-incorporated short DNA sequence, 5'-TCACAXTTCCA-3', shows that the UBP becomes planar and almost resembles the natural base pairs. We show that dispersion interactions between the UBP and the natural base pairs within the DNA sequence (intrastrand) rather than the interactions within a UBP (interstrand) lead to the stabilization of an UBP-incorporated DNA. This is also supported by the fact that when a void is incorporated inside the same sequence replacing the UBP the structure of the modified DNA is significantly distorted. Therefore, we believe that the 5SICS–NaM pair creates a minimal perturbation to the overall structure of DNA. The strong H-bond stabilization of the remaining natural base pairs in the sequence over-

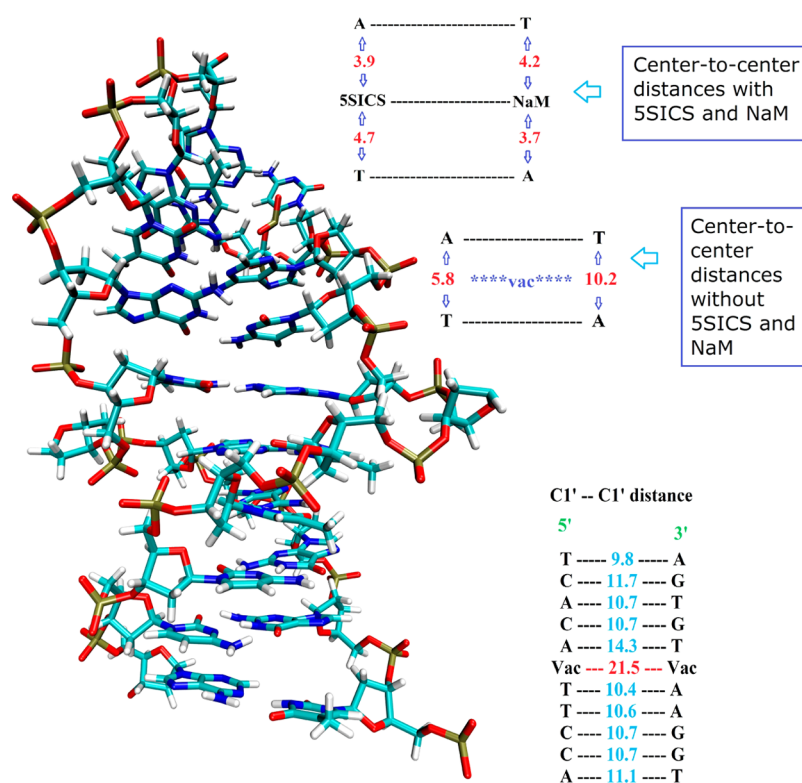


**Figure 6.** MD snapshot of the DNA sequence with a void at the location of the UBP. The C1'–C1' distance for this void@DNA is shown along with its center-to-center distance, which is compared with UBPA@DNA.

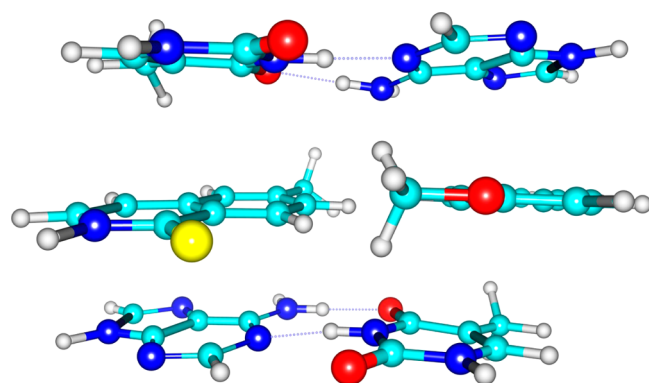


**Figure 7.** Structure of the free UBPA flanked between two AT pairs as retrieved from the equilibrated MD simulation of UBPA inserted DNA sequence.

compensates the loss stacking interactions of the UBPA and therefore enforces a planar configuration. Clearly, the combined effects of backbone and the neighboring stacked natural bases, which are themselves paired by strong hydrogen bonding, ensure that UBPA almost resembles the natural base pairs, which we conjecture leads to recognition by the DNA unzipping enzymes and therefore sustains and replicates just like natural genetic material.

## ■ ASSOCIATED CONTENT

### ● Supporting Information

Cartesian coordinates, energies, harmonic frequencies for all the structures reported, additional calculations, and complete ref 17. The Supporting Information is available free of charge on the ACS Publications website at DOI: 10.1021/acs.jpcb.5b03293.

## ■ AUTHOR INFORMATION

### Corresponding Author

\*E-mail: spad@iacs.res.in. Tel: +91-33-24734971.

### Notes

The authors declare no competing financial interest.

## ■ ACKNOWLEDGMENTS

A.D. thanks DST and INSA for partial funding. S.J. thanks CSIR for JRF. We thank Dr. Justin A. Lemkul for fruitful discussions.

## ■ REFERENCES

- (1) Malyshev, D. A.; Dhami, K. A.; Lavergne, T.; Chen, T.; Dai, N.; Foster, J. M.; Corrêa, I. R., Jr.; Romesberg, F. E. A Semi-Synthetic Organism with an Expanded Genetic Alphabet. *Nature* **2014**, *509*, 385–388.
- (2) Kimoto, M.; Yamashige, R.; Matsunaga, K.; Yokoyama, S.; Hirao, I. Generation of High-Affinity DNA Aptamers Using an Expanded Genetic Alphabet. *Nat. Biotechnol.* **2013**, *31*, 453–457.
- (3) Chen, T.; Shukoor, M. L.; Chen, Y.; Yuan, Q.; Zhu, Z.; Zhau, Z.; Gulbakan, B.; Tan, W. Aptamer-Conjugated Nanomaterials for Bioanalysis and Biotechnology Applications. *Nanoscale* **2011**, *3*, 546–556.
- (4) Lu, C.; Wilner, B.; Wilner, I. DNA Nanotechnology: From Sensing and Machines to Drug-Delivery Systems. *ACS Nano* **2013**, *7*, 8320–8332.
- (5) Jissy, A. K.; Datta, A. Design and Applications of Nanocanonical DNA Base Pairs. *J. Phys. Chem. Lett.* **2014**, *5*, 154–166.
- (6) Yang, Z.; Chen, F.; Alvarado, J. B.; Benner, S. A. Amplification, Mutation, and Sequencing of a Six-Letter Synthetic Genetic System. *J. Am. Chem. Soc.* **2011**, *133*, 15105–15112.
- (7) Morales, J. C.; Kool, E. T. Efficient Replication between Non-Hydrogen-Bonded Nucleoside Shape Analogs. *Nat. Struct. Biol.* **1998**, *5*, 950–954.



- (8) Yamashige, R.; Kimoto, M.; Takezawa, Y.; Sato, A.; Mitusui, T.; Yokoyama, S.; Hirao, I. Highly Specific Unnatural Base Pair Systems as a Third Base Pair for PCR Amplification. *Nucleic Acid Res.* **2012**, *40*, 2793–2806.
- (9) Idili, A.; Vallee-Belisle, A.; Ricci, F. Programmable pH-Triggered DNA Nanoswitches. *J. Am. Chem. Soc.* **2014**, *136*, 5836–5839.
- (10) Lee, J. A.; DeRosa, M. C. A pH-driver DNA Switch Based on the A+G mispair. *Chem. Commun.* **2010**, *46*, 418–420.
- (11) Jissy, A. K.; Datta, A. Designing Molecular Switches Based on DNA-Base Mismatching. *J. Phys. Chem. B* **2010**, *114*, 15311–15318.
- (12) Zhao, Y.; Schultz, N. E.; Truhlar, D. G. Design of Density Functional by Combining the Method of Constraint Satisfaction with Parametrization for Thermochemistry, Thermochemical Kinetics, and Noncovalent Interactions. *J. Chem. Theory Comput.* **2006**, *2*, 364–382.
- (13) Hohenstein, E. G.; Chill, S. T.; Sherrill, C. D. Assessment of the Performance of the M05-2X and M06-2X Exchange-Correlation Functional for Noncovalent Interactions in Biomolecules. *J. Chem. Theory Comput.* **2008**, *4*, 1996–2000.
- (14) Jissy, A. K.; Ashik, U. P. M.; Datta, A. Nucleic Acid G-quartets: Insights into Diverse Patterns and Optical properties. *J. Phys. Chem. C* **2011**, *115*, 12530–12546.
- (15) Chai, J. D.; Head-Gordon, M. Long-range Corrected Hybrid Density Functional with Damped Atom-Atom Dispersion Corrections. *Phys. Chem. Chem. Phys.* **2008**, *10*, 6615.
- (16) Grimme, S. Density Functional Theory with London Dispersion Corrections. *WIREs Comput. Mol. Sci.* **2011**, *1*, 211–228.
- (17) Frisch, M. J.; et al. *Gaussian 09*, revision D. 01; Gaussian, Inc.: Wallingford, CT, 2013.
- (18) Neese, F. The ORCA Program System. *Wiley Interdiscip. Rev.: Comput. Mol. Sci.* **2012**, *2*, 73–78.
- (19) Vanommeslaeghe, K.; Hatcher, E.; Acharya, C.; Kundu, S.; Zhong, S.; Shim, J.; Darin, E.; Guvench, O.; Lopes, P.; Vorobyov, I.; MacKerell, A. D., Jr. CHARMM general force field: A Force Field for Drug-like Molecules Compatible with the CHARMM All-Atom Additive Biological Force Fields. *J. Comput. Chem.* **2010**, *31*, 671–690.
- (20) Banavali, N. K.; MacKerell, A. D., Jr. All-Atom Empirical Force Field for Nucleic Acids: II. Applications to Molecular Dynamics Simulations of DNA and RNA in Solution. *J. Comput. Chem.* **2000**, *21*, 105–120.
- (21) *make-na*; <http://structure.usc.edu/make-na/> (accessed September 25, 2014).
- (22) Macke, T. J.; Case, D. A. Modeling Unusual Nucleic Acid Structures. In *Molecular Modeling of Nucleic Acids*; Leontes, N. B., Santa Lucia, J., Jr., Eds.; American Chemical Society: Washington, DC, 1998; pp 379–393.
- (23) Phillips, J. C.; Barun, R.; Wang, W.; Gumbart, J.; Tajkhorshid, E.; Villa, E.; Chipot, C.; Skeel, R. D.; Kalé, L.; Schulten, K. Scalable Molecular Dynamics with NAMD. *J. Comput. Chem.* **2005**, *26*, 1781–1802.
- (24) Humphrey, W.; Dalke, A.; Schulten, K. VMD – Visual Molecular Dynamics. *J. Mol. Graphics* **1996**, *14*, 33.
- (25) Bondi, A. van der Waals Volumes and Radii. *J. Phys. Chem.* **1964**, *68*, 441–451.
- (26) Riley, K. E.; Hobza, P. On the importance and Origin of Aromatic Interactions in Chemistry and Biodisciplines. *Acc. Chem. Res.* **2013**, *46*, 927–936.
- (27) Berka, K.; Laskowski, R.; Riley, K. E.; Hobza, P.; Vondrasek, J. Representative Amino Acid Side Chain Interactions in Proteins. A Comparison of Highly Accurate Correlated ab-initio Quantum Chemical and Empirical potential procedures. *J. Chem. Theor. Comput.* **2009**, *5*, 982–992.
- (28) Hobza, P.; Selze, H. L.; Schlag, E. W. Potential Energy Surface for the Benzene Dimer. Results ab initio CCSD(T) Calculation Show Two nearly Isoenergetic Structures: T-Shaped and Parallel-Displayed. *J. Phys. Chem.* **1996**, *100*, 18790–18794.
- (29) Sinnokrot, M. O.; Valeev, E. F.; Sherrill, C. D. Estimates of the Ab-initio Limit for  $\pi$ - $\pi$  Interactions: The Benzene Dimer. *J. Am. Chem. Soc.* **2002**, *124*, 10887–10893.
- (30) Riley, K. E.; Hobza, P. Noncovalent Interactions in Biochemistry. *Wiley Interdiscip. Rev.: Comput. Mol. Sci.* **2011**, *1*, 3–17.
- (31) Grimme, S.; Goerigk, L.; Fink, R. F. Spin-component-scaled Electron Correlation Methods. *Wiley Interdiscip. Rev.: Comput. Mol. Sci.* **2012**, *2*, 886–906.
- (32) Sponer, J.; Jureka, P.; Marchan, I.; Luque, F. J.; Orozco, M.; Hobza, P. Nature of Base Stacking: Reference Quantum-Chemical Stacking Energies in Ten Unique B-DNA Base-Pair Steps. *Chem.—Eur. J.* **2006**, *12*, 2854–2865.
- (33) Reha, D.; Hock, M.; Hobza, P. Exceptional Thermodynamic Stability of DNA Duplexes Modified by Nonpolar Base Analogues Is due to Increased Stacking Interactions and Favorable Solvation: Correlated Ab Initio Calculations and Molecular Dynamics Simulations. *Chem.—Eur. J.* **2006**, *12*, 3587–3595.
- (34) Jurecka, P.; Hobza, P. True Stabilization Energies for the Optimal Planar hydrogen-Bonded and Stacked Structures of Guanine—Cytosine, Adenine—Thymine, and Their 9-and 1-Methyl Derivatives: Complete basis Set Calculations at the MP2 and CCSD(T) Levels and Comparison with Experiment. *J. Am. Chem. Soc.* **2003**, *125*, 15608–15613.
- (35) Cossi, M.; Rega, N.; Scalmani, G.; Barone, V. Energies, Structures, and Electronic Properties of Molecules in solution with the C-PCM solvation model. *J. Comput. Chem.* **2003**, *24*, 669–681.
- (36) Poater, J.; Swart, M.; Guerra, C. F.; Bickelhaupt, F. M. Selectivity in DNA Replication. Interplay of Steric shape, Hydrogen bonds,  $\pi$ -stacking and Solvent effects. *Chem. Commun.* **2011**, *47*, 7326–7328.
- (37) Poater, J.; Swart, M.; Guerra, C. F.; Bickelhaupt, F. M. Solvent Effects on Hydrogen Bonds in Watson-Crick, Mismatched, and Modified DNA base pairs. *Comput. Theor. Chem.* **2012**, *998*, 57–63.
- (38) Jissy, A. K.; Konar, S.; Datta, A. Molecular Switching Behavior in Isosteric DNA Base Pairs. *ChemPhysChem* **2013**, *14*, 1219–1226.
- (39) Compared with the gas-phase BSSE-corrected binding energies, the free energy of association at 300 K is significantly lower due to the entropic penalty. Similar observations have also been made regarding the association of natural bases in aqueous media. Dang, L. X.; Kollman, P. A. Molecular Dynamics Study of the Free Energy of Association of 9-methyladenine and 1-methylthymine Bases in Water. *J. Am. Chem. Soc.* **1990**, *112*, 503–507.
- (40) Vreven, T.; Byun, K. S.; Komáromi, I.; Dapprich, S.; Montgomery, J. A., Jr.; Morokuma, K.; Frisch, M. J. Combining Quantum Mechanics Methods with Molecular Mechanics Methods in ONIOM. *J. Chem. Theory Comput.* **2006**, *2*, 815–826.
- (41) Banavali, N. K.; MacKerell, A. D., Jr. All-Atom Empirical Force Field for Nucleic Acids: II. Application to Molecular Dynamics Simulations of DNA and RNA in Solution. *J. Comput. Chem.* **2000**, *21*, 105–120.
- (42) Betz, K.; Malyshev, D. A.; Lavergne, T.; Welte, W.; Diederichs, K.; Dwyer, T. J.; Ordoukhanian, P.; Romesberg, F. E.; Marx, A. KlenTaq Polymerase Replicates Unnatural Base Pairs by Inducing a Watson-Crick Geometry. *Nat. Chem. Biol.* **2012**, *8*, 612–614.
- (43) Betz, K.; Malyshev, D. A.; Lavergne, T.; Welte, W.; Diederichs, K.; Romesberg, F. E.; Marx, A. Structural Insights into DNA Replication without Hydrogen Bonds. *J. Am. Chem. Soc.* **2013**, *135*, 18637–18643.